Texture Analysis for Wind Turbine Fault Detection

Luis E. MUJICA , Magda RUIZ, Leonardo ACHO, Santiago ALFÉREZ, Christian TUTIVÉN, Yolanda VIDAL, José RODELLAR

Department of Mathematics, Escola d'Enginyeria de Barcelona Est (EEBE), Universitat Politècnica de Catalunya (UPC) BARCELONATECH, Barcelona, Spain
{luis.eduardo.mujica, magda.ruiz, leonardo.acho, santiago.alferez, christian.tutiven, yolanda.vidal, jose.rodellar}@upc.edu

Key words: Smart structures, Modeling, Experimental validation, Industrial applications, Texture analysis, Digital image processing.

Abstract

The future of wind energy industry passes through the use of larger and more flexible wind turbines in remote locations, which are increasingly offshore to benefit stronger and more uniform wind conditions. Cost of operation and maintenance of offshore wind turbines is among 15-35% of the total cost. From this, 80% comes from unplanned maintenance due to different faults in the wind turbine components. Thus, an auspicious way to contribute to the increasing demands and challenges is by applying low-cost advanced fault detection schemes. This work proposes a new method for fault detection of wind turbine actuators and sensors faults in variable-speed wind turbines. For this purpose, time domain signals acquired from the operating wind turbine are converted into two-dimensional matrices to obtain gray-scale digital images. Then, the image pattern recognition is processed getting texture features under a multichannel representation. In this work, four types of texture features are used: statistical, wavelet, granulometric and Gabor features. Then, the most significant features are selected with the conditional mutual criterion. Finally, the fault detection is performed using an automatic classification tool. In particular, a 10-fold cross validation is used to obtain a more generalized model and evaluate the classification performance. In this way, the healthy and faulty conditions of the wind turbine can be detected. Coupled non-linear aero-hydro-servo-elastic simulations of a 5MW offshore type wind turbine are carried out for several fault scenarios. The results show a promising methodology able to detect the most common wind turbine faults.

1   INTRODUCTION

Offshore wind farms promise to become an important source of energy in the near future. However, their operation and maintenance is more difficult and expensive than for equivalent onshore wind farms. The current reliability and failure modes of commercial offshore wind turbines are such that a 'no maintenance' strategy is not a viable option. Improved preventive and corrective maintenance schemes will become crucial for economic exploitation of offshore wind power. Thus, a promising way to contribute is by applying low-cost advanced fault detection schemes. In this regard, this work proposes a new fault detection method that uses on-line SCADA (supervisory control and data acquisition) data already available at an industrial wind turbine.

Several methods for fault detection have been proposed in different engineering fields. These methods can be mainly classified according to their procedure: namely model based, signal based and data based. In all of them, the fundamental part is the signal processing. Wherein, the goal in signal processing is to highlight the signal behaviour. However recent applications have begun to use digital images for fault detection and pattern recognition. Shahriar et. al. proposes fault diagnosis of induction motors using digital grayscale images [1]. On the other hand, the authors have experience in fault detection of wind turbines based on data [2] and classification of abnormal cells images using texture features [3]. Thus, merging these two areas of knowledge, a methodology for fault diagnosis in wind turbines using digital image processing is proposed.

In this work, the benchmark model for wind turbine fault detection, isolation and accommodation proposed in [4] is used. The aim of the benchmark model is to provide a common ground to test and compare different methods taking into account the most common faults in megawatt-sized wind turbines. In this work, once the signals are stored, they are converted in grayscale images. Next, the texture feature extraction is performed. It computes the visual patterns that composes an image, which can be regarded as a similarity grouping in an image. Because of the high computational cost associated to the use of all the texture features, this number has to be reduced. This is achieved giving priority to the most relevant and less redundant texture features. Finally, a process of training and validation of the classification technique is developed. Thus the methodology for fault detection is outlined and calibrated.

This work is organized as follows: the benchmark model for wind turbines is explained in Section 2. Then, the overall design of the methodology, including the stages that comprise it, are reported in Section 3. Next, results are discussed in Section 4. Finally, conclusions are drawn in Section 5.

2 BENCHMARK MODEL

This section gives a very brief review of the used benchmark model and the studied fault scenarios. For a comprehensive explanation, see [4].

In the benchmark model, the NREL (National Renewable Energy Laboratory) offshore 5-MW wind turbine simulated with the FAST (fatigue, aerodynamic, structures, and turbulence) software is used [5][6]. Models for the pitch and generator-converter actuators are added to the FAST code following [4]. Sensor and actuator faults are considered as described in Table I. These faults, selected by the benchmark, cover different parts of the wind turbine, different fault types, and different levels of severity.

Fault	Type	Description
1	Pitch actuator	High air content in oil/ Pump wear/ Hydraulic leakage
2	Generator speed sensor	Scaling (gain factor equal to 1.2)
3	Pitch angle sensor	Stuck (fixed value equal to 5 deg or 10 deg)
4	Torque actuator	Offset (offset value equal to 2000Nm)

Table I: Fault scenarios

Most industrial wind turbines are manufactured with an integrated system that can monitor various turbine parameters. These monitored data are collated and stored via a supervisory control and data acquisition (SCADA) system that archives the information in a convenient manner. Table II presents the assumed available data on a MW-scale industrial wind turbine that are used in this work.

Number	Sensor type	Units
1	Generated electrical power	kW
2	Rotor speed	rad/s
3	Generator speed	rad/s
4	Generator torque	Nm
5	First pitch angle	deg
6	Second pitch angle	deg
7	Third pitch angle	deg
8	Fore-aft acceleration at tower bottom	m/s^2
9	Side-to-side acceleration at tower bottom	m/s^2
10	Fore-aft acceleration at mid-tower	m/s^2
11	Side-to-side acceleration at mid-tower	m/s^2
12	Fore-aft acceleration at tower top	m/s^2
13	Side-to-side acceleration at tower top	m/s^2

Table II: Assumed available measurements. These sensors are representative of the SCADA (supervisory control and data acquisition) data available in a MW-scale industrial wind turbine.

3 DESIGN OF A METHODOLOGY FOR WIND TURBINE FAULT DIAGNOSIS

MW-scale industrial wind turbines are huge structures generally installed in remote locations in which operation and maintenance (O&M) plays an important role. In this work, a new methodology for fault detection is proposed. Several cases for each one of the wind turbine operating conditions (normal operation – Normal– and faulty – Faults 1 to 4–) are simulated using the benchmark model (See Section 2). In each simulation, the variables shown in Table II are measured and converted into digital images (Section 3.1). In consequence, each case is defined by 13 digital images. The next step is to get the texture features to characterize the differences between the operating wind turbine conditions: normal or faulty. From each image, 65 features are extracted. Then, a total of 845 features define each case (Section 3.2). This high number of features complicates the fault detection leading to a high computational cost. Therefore, the most significant features are selected with the conditional mutual criterion (Section 3.3) leading to only 100 texture features to be used as inputs to the classifier. Finally, a 10-fold cross validation is used to obtain a more generalized model and evaluate the classification performance. Hence, a set of images is selected for training and the rest is used to validate the classification technique (Section 3.4). As final outcome, a methodology based on images for detection and classification of different operating conditions (normal or faulty) in wind turbines is obtained. A general scheme of the methodology is presented in Figure 1.
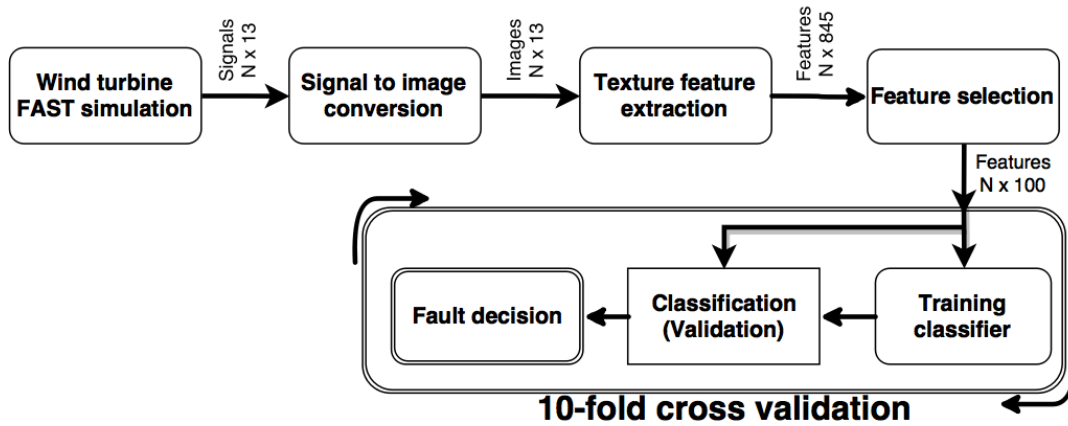
Figure 1.
Proposed methodology for wind turbine fault diagnosis.

3.1 Signal to image conversion

Following the criterion described in [1], the chosen image size is 128 × 128 pixels. An image per signal is generated (Figure 2). After the transient period, the first 128 data-points (Figure 2A) determine the first row of gray-scale image (Figure 2B). Immediately after, the next 128 data-points determine the second row and so on (Figure 2B). In this work, 140 images for Normal, 120 for Fault 1, 40 for Fault 2, 80 for Fault 3 and 40 for Fault 4 are generated. Given that the time step for simulation of the wind turbine benchmark model is 0.0125s, almost 24h of simulation of the wind turbine are needed to obtain all these data.
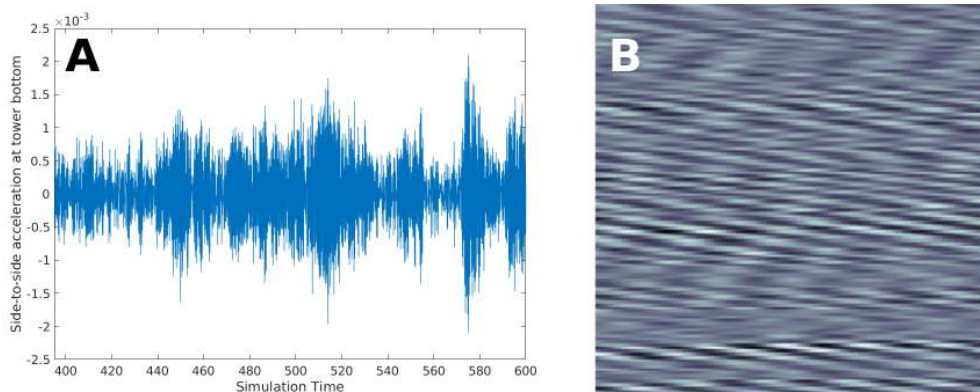

Figure 2. Example of the signal to image conversion process for a case with fault 2. A: original signal of the side-to-side acceleration at mid-tower variable; B: image result after the conversion.

3.2 Texture feature extraction

Texture is an important issue in image processing. The idea to use texture features comes from the innate human ability to recognize textural differences using the vision and touch. Texture in digital image is defined by the uniformity, density, thickness, roughness, regularity, intensity, the directionality, the pixel tone and their spatial relationships, among others. The main goal of the feature extraction is to get quantitative measures in order to identify different texture patterns. Several procedures to analyze the texture of a digital image can be found in the literature [7]. In this work, four types of texture features are used: statistical, wavelet, granulometric and Gabor features. Figure 3 shows a representative scheme of the extracted texture features.
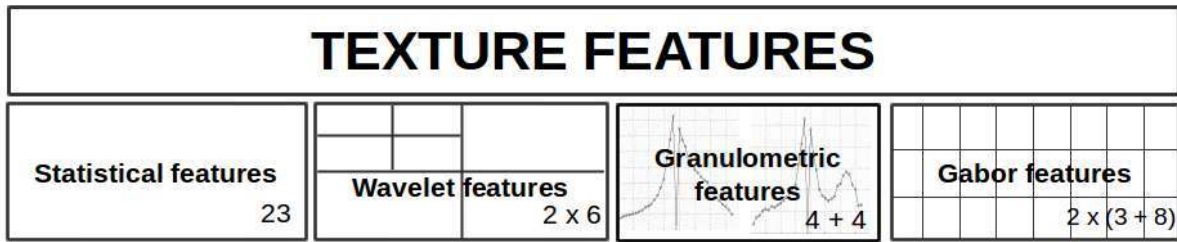
4

Figure 3. Scheme of the texture features.

Statistical features: These can be divided into first and second-order statistical features. The first order features are based on the histogram of the digital image: mean, standard deviation, skewness, kurtosis, energy and entropy are used in this work. The second-order statistical features are based on the gray level co-occurrence matrix: uniformity, contrast, homogeneity, correlation, sum average, sum variance, sum entropy, entropy, difference variance, difference entropy, information measures of correlation 1 and 2, maximal correlation coefficient and maximum probability are implemented here [8]. In addition, two more features are also added: cluster shade and cluster prominence [9].

Wavelet features: The original image (Figure 4A) is decomposed into 4 sub-images using the discrete wavelet transform, as it is shown in Figure 4B. As a result, an approximation of the image and three highlighted versions of the horizontal, vertical and diagonal details are obtained. This process is repeated in a second level decomposition over the above first approximation image to obtain three more detailed sub-images and another level of the approximation (see Figure 4C). On these 6 detail sub-images, mean and standard deviation are calculated to obtain 12 wavelet features [10] .
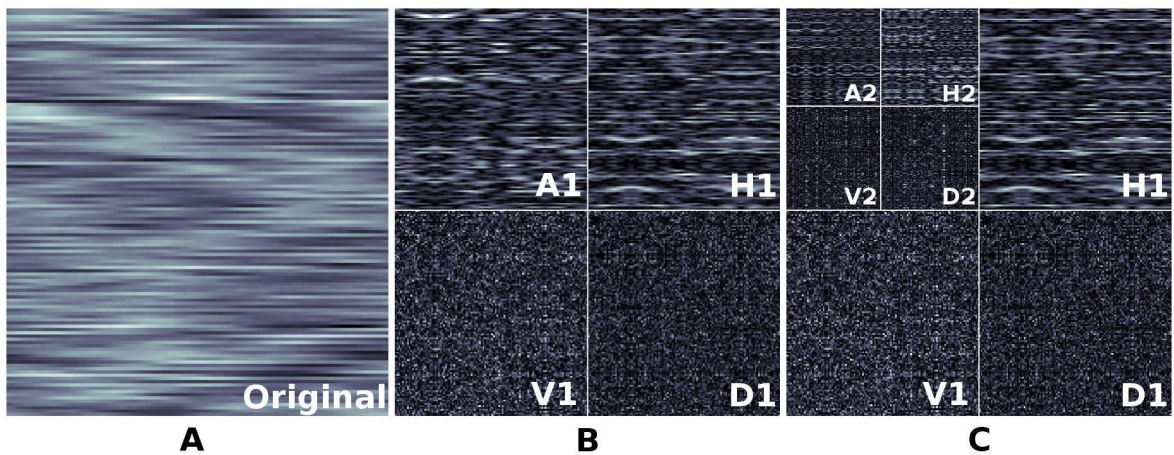

Figure 4. Application example of the discrete wavelet transform on an image corresponding to the side-to-side acceleration at tower bottom (m/s^2) variable. A: original image; B: first level wavelet decomposition; C: second level wavelet decomposition.

Granulometric features: They are determined from the granulometric curve and the pseudo-granulometric curve. Both curves represent the size distribution of the bright and dark granules on the image. The granulometric curve is calculated by successive mathematical morphological operations of opening and closing. The pseudo-granulometric curve is calculated by successive operations of erosion and dilation. Four simple features were used to obtain information about each of the two curves: mean, standard deviation, skewness and kurtosis [11][12].

Gabor features: These features are obtained from different versions of the image processed by Gabor filters. These filters are related to the function of simple cells in the visual cortex of primates. Gabor functions depend up to 7 parameters, of which 5 are left constant (in this study) and the remaining two, the wavelength λ and the orientation Θ, are variable [13]. In this work, a bank of 28 filters corresponding to three wavelengths $\lambda = \{8, 12, 15\}$ and eight orientations between 22.5º and 180º are used (Figure 5). With this filter bank, three rotation-invariant Gabor responses are obtained, summing for each wavelength λ all the filtered images corresponding to the 8 orientations (the rightmost column of Figure 5). In the same way, eight scale-invariant Gabor responses are obtained, summing for each orientation Θ all the filtered images corresponding to the 3 wavelengths (the bottom row of Figure 5) [14]. Therefore, a total of 11 Gabor image responses are used. For each combined response, the mean and the standard deviation are calculated.
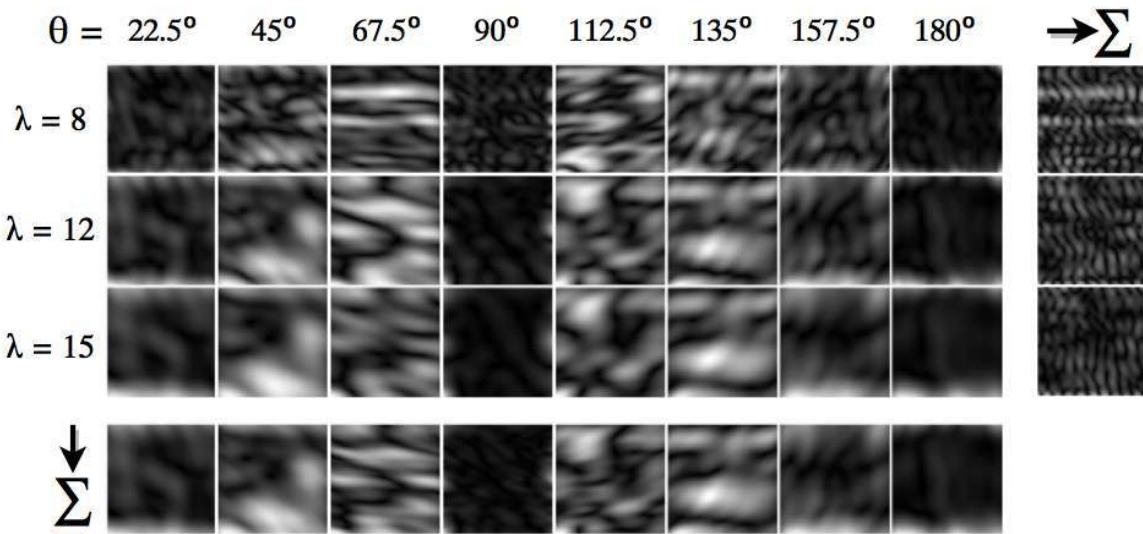

Figure 5. Gabor responses for the side-to-side acceleration at mid-tower image variable for a case with fault 2

In summary, 65 texture features are extracted for each image. Since there are 13 images, a total of 845 features by image are obtained to describe each case.

3.3 Texture feature selection

When many features are extracted, the complexity of the problem description becomes higher, making difficult to build a good classification system. Feature selection defines a topic commonly used in machine learning to select the more significant features. Feature selection allows to improve the classification performance, it makes faster and more profitable classifiers, it provides a better understanding of the data processing and avoids the curse of dimensionality. In this work, the information theoretic feature selection with the conditional mutual info maximization (CMIM) criterion is used [15]. The features are sorted from the most relevant (and less redundant) to the less relevant (and most redundant). Then, the first 100 features are selected.

3.4 Fault classification

The most important texture features are used as inputs to the classifier. Here, two classification techniques are compared: support vector machines (SVM) and ensemble learning methods. Additionally, a 10-fold cross-validation is implemented to ensure that the results are independent from the data set. In this way, 10 repetitions are performed where one set of images are randomly selected (considering a representative quantity for each operation condition –stratified sampling–) as training set and the remaining ones are used for the validation. The best fault detection and classification is obtained using bootstrap aggregation as ensemble learning method with decision trees as weak learners (Bagged Trees). This technique fits the base classifiers, in this work there are 5 classes: Normal and Faults 1 to 4. Next, each image is randomly located on these classes and then their individual predictions are aggregated, to give a final prediction either by voting or by averaging [16].

4. RESULTS AND DISCUSSION

The dispersion and symmetry of the most relevant features can be observed using boxplot. Thereby, the boxplots that provide an overview of the contribution for the four best features are shown in Figure 6, in which the outliers have not been considered. The first feature is the mean of the scale-invariant Gabor texture for an angle of 135º, obtained from the Generated Power variable (Figure 6A). In this plot, Fault 2 (generator speed sensor) is undoubtedly separated from the other classes. Fault 4 (torque actuator) is slightly distanced from the rest as well. The second feature is the standard deviation of the first vertical detail from wavelet decomposition, obtained from the third pitch angle variable (Figure 6B). This plot shows that Fault 1 (pitch actuator) is clearly isolated from the rest. From the rotor speed original variable, the third most relevant feature (correlation) is obtained (Figure 6C). The fourth relevant feature is the information measure of correlation 1, obtained from the generated power (Figure 6D). In C and D subplots, Fault 3 (pitch angle sensor) is mildly separated from the others classes. Comparing the first four best features, it can be observed that the capacity to distinguish between classes is gradually lost. In consequence, 100 texture features are chosen as inputs to the classification tools.

Once the feature selection is performed, the determination process for the best classifier is developed. Therefore, all the cases (normal and faulty cases) defined by the 100 texture features are randomly partitioned into ten sets (10-fold cross validation). 378 cases determine the training set and 42 the validation set for any iteration. Next, in each iteration the training set is used to train the classifier and the validation set is used to quantify the classification accuracy, where the percentage of data correctly classified defines the accuracy. Additionally, different classification techniques have been implemented, including SVM and bagged trees. In Figure 7A and 7B, results for bagged trees and SVM classification techniques (respectively) are showed. These results are presented as confusion matrices where the rows are the true classification and the columns are the prediction of the technique. There, each cell represents the number of classifications in each class (they are shown as percentages with respect to the total number of true cases for each row).
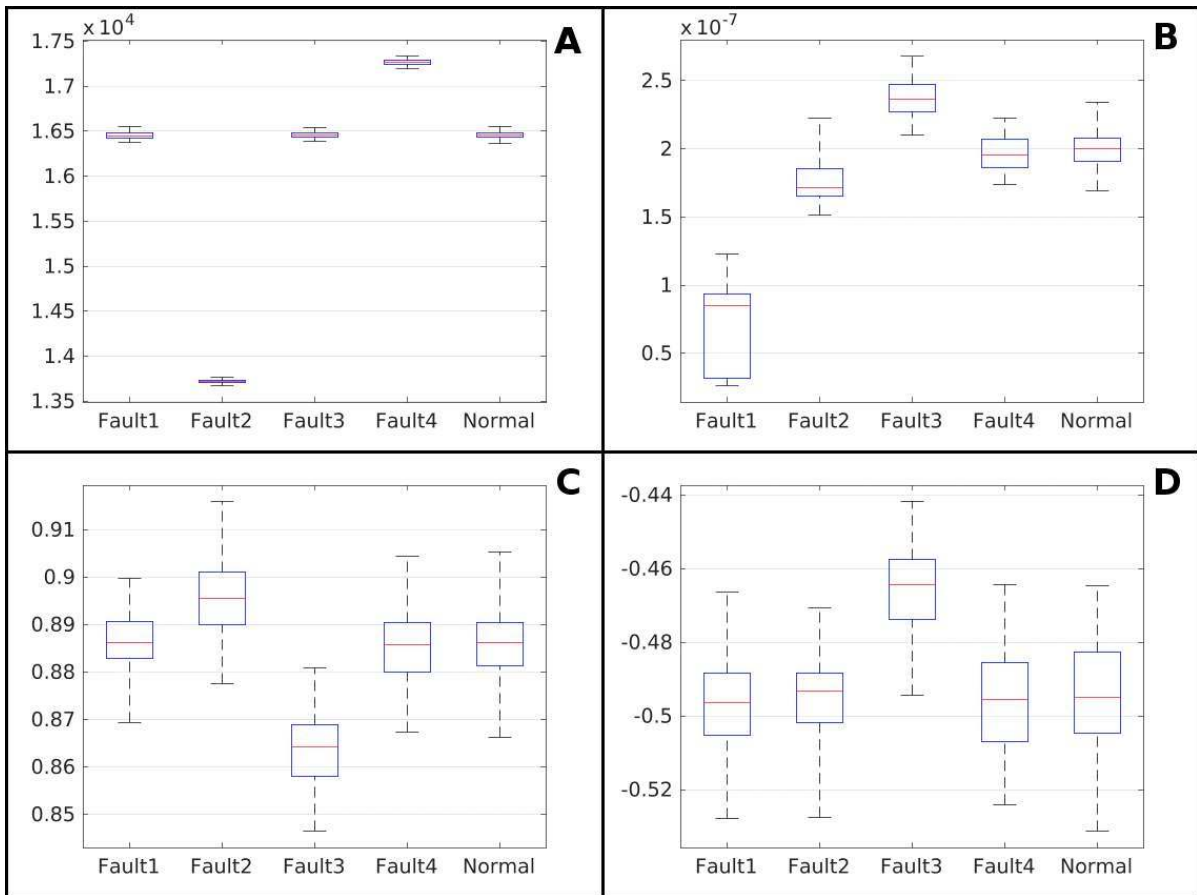
Figure 6. Boxplots for the four most relevant texture features: A: First feature. B: Second feature. C: Third feature. D: Fourth feature.
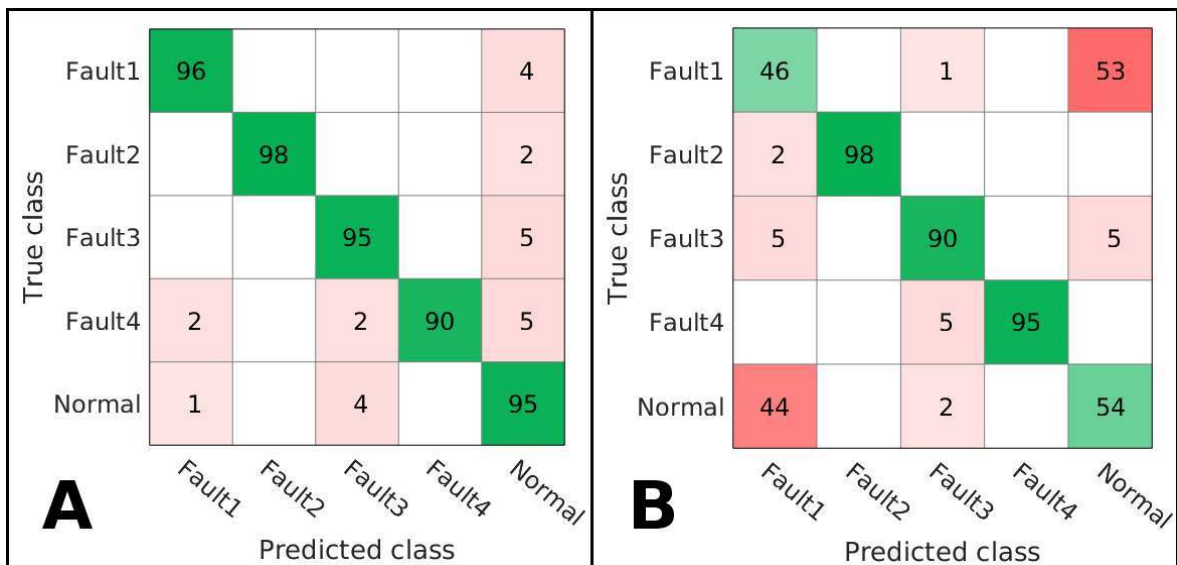

Figure 7. Performance classification results for the 10-fold cross validation process: A: Bagged tree. B: Support Vector Machine.

Figure 7A shows the results using Bagged trees classifier. The overall accuracy is a golden 95%. It uses 40 supervised learners (ensemble ideology) allowing more flexibility among the classes with a low computational cost. For example, 98% of the cases with the Fault 2 condition are classified correctly and only 2% are classified as the normal condition.

The SVM classifier uses a linear Kernel function with a box constraint level of 1. Since there are more than two classes (Normal and Fault 1,2,3,4), the comparison is performed using the multiclass method one vs one. Figure 7B shows that this classifier does not distinguish properly between classes Fault 1 and Normal: 53% of the cases belonging to Fault 1 are classified as Normal. Similarly, 44% of Normal cases are incorrectly classified as Fault 1. Thus, the SVM overall classification accuracy is poorly a 66.7%.

In a deep comparison of both classification techniques, Fault 2 has the same accuracy, while Fault 1 and Normal cases are better classified using Bagged trees. As opposed, Fault 4 has an increased classification using the SVM technique. In conclusion, and despite the complex configuration of the Bagged trees, it has a lesser computational cost and gives better accuracy than the SVM technique.

5. CONCLUSIONS

The main challenges of the wind turbine fault detection lie in its nonlinearity and unknown disturbances (such as the wind). Direct diagnosis of the wind turbine condition can not be done from the available SCADA data. However, in this work, numerical simulations (with a well-known benchmark wind turbine) show that the proposed method is capable of classifying between normal operation or Fault 1 to Fault 4 with a remarkable overall accuracy of 95%. It is noteworthy that the studied faults are the most common in real MW-scale industrial wind turbines, thus the obtained accuracy is promising. For future work, a complete fault detection, isolation and reconfigurable control strategy in response to faults will be developed.

REFERENCES

[1] Shahriar R.; Ahsan T.; Chong U. Fault diagnosis of induction motors utilizing local binary patter-based texture analysis. *EURASIP Journal on Image and Video Processing* 2013:**29**.

[2] Pozo, F. and Vidal, Y. Wind Turbine Fault Detection through Principal Component Analysis and Statistical Hypothesis Testing. *Energies*. 09-00003. 2016

[3] Alférez, S.; Merino, A,; Mujica, L.E.; Ruiz, M.; Bigorra, L. and Rodellar, J. Automatic recognition of atypical lymphoid cells from peripheral blood by digital image analysis. *American Journal of Clinical Pathology*, Vol. **143(2)**, pp. 168-176, 2015

[4] Odgaard, P.; Johnson, K. Wind Turbine Fault Diagnosis and Fault Tolerant Control - an Enhanced Benchmark Challenge. *Proc. of the 2013 American Control Conference–ACC,(Washington DC, USA),* pp. 1–6. 2013,.

[5] Jonkman, J.M.; Butterfield, S.; Musial, W.; Scott, G. Definition of a 5-MW reference wind turbine for offshore system development. Technical report, National Renewable Energy Laboratory, Golden, Colorado, 2009. NREL/TP-500-38060.

[6] Jonkman, J. NWTC Computer-Aided Engineering Tools (FAST), Last modified 28-October- 2013.

[7] A. Materka, M. Strzelecki, Texture Analysis Methods – A Review, Technical. University of Lodz, Institute of Electronics, COST B11 report, Brussels 1998

[8] Haralick RM, Shanmugam K, Dinstein I. Textural features for image classification. *IEEE Trans Syst Man Cybern* 1973;3:610-621.

[9] Albregtsen F. Statistical Texture Measures Computed from Gray Level Coocurrence Matrices. Image Processing Laboratory, Department of Informatics, University of Oslo 1995.

[10] Arivazhagan S, Ganesan L. Texture classification using wavelet transform. *Pattern Recognit Lett* 2003;24:1513-1521.

[11] Angulo J. A mathematical morphology approach to cell shape analysis. In: Bonilla LL, Moscoso M, Platero G, et al., eds. Progress in Industrial Mathematics at ECMI 2006.Vol 12. Berlin, Heidelberg: Springer; 2008:2-6.

[12] Alférez, S.; Merino, A,; Mujica, L.E.; Ruiz, M.; and Rodellar, J. Automatic classification of atypical lymphoid B cells using digital blood image processing. *International Journal Lab Hematology* 2014;36:472-80.

[13] Kruizinga P, Petkov N. Nonlinear Operator for Oriented Texture. 1999;8:1395-1407.

[14] Han J, Ma KK. Rotation-invariant and scale-invariant Gabor features for texture image retrieval. *Image and Vision Computing* 2007;25:1474-1481.

[15] Brown G, Pocock A, Zhao M-J, et al. Conditional likelihood maximisation: a unifying framework for information theoretic feature selection. *Journal of Machine Learning Research* 2012;13:27-66.

[16] L. Breiman, "Bagging predictors", *Machine Learning*, 24(2), 123-140, 1996.